

Use of a Stopped-flow Technique to measure the Rate Constants at Room Temperature for Reactions between the Nitrate Radical and Various Organic Species

Andrew A. Boyd, Carlos E. Canosa-Mas, A. Douglas King, Richard P. Wayne* and Mark R. Wilson
Physical Chemistry Laboratory, University of Oxford, South Parks Road, Oxford OX1 3QZ, UK

A stopped-flow apparatus, in which NO_3 was detected by optical absorption at $\lambda = 662 \text{ nm}$, has been used to measure overall rate constants at room temperature for reaction of NO_3 in systems involving ethene, simple alkanes and chlorinated methanes. Modelling of the reaction with ethene led to a rate constant for the primary step of $(1.7 \pm 0.5) \times 10^{-16} \text{ cm}^3 \text{ molecule}^{-1} \text{ s}^{-1}$. However, for H-atom abstraction by NO_3 from the saturated organic species, the extensive and largely unquantified secondary chemistry occurring over reaction times of 5–20 s meant that only upper limits for the primary rate constants could be accurately assessed (the stoichiometric factor being assumed to be two or more). The values thus obtained at room temperature were (in units of $10^{-17} \text{ cm}^3 \text{ molecule}^{-1} \text{ s}^{-1}$) 2.7 ± 0.2 , 4.8 ± 1.7 , 60 ± 10 , 0.85 ± 0.25 , 0.48 ± 0.10 and 6.0 ± 0.5 for ethane, propane, isobutane (2-methylpropane), acetone, dichloromethane and chloroform. For the reactions of NO_3 with ethane and propane, modelling of the kinetics led to estimates of lower limits of the primary rate constants of (1.1 ± 0.2) and $(2.2 \pm 0.2) \times 10^{-17} \text{ cm}^3 \text{ molecule}^{-1} \text{ s}^{-1}$. No reaction was observed between NO_3 and methane or chloromethane, suggesting upper limits (based on the noise levels) for the overall rate constants of these reactions of 8×10^{-19} and $1 \times 10^{-18} \text{ cm}^3 \text{ molecule}^{-1} \text{ s}^{-1}$.

The nitrate radical is formed in the atmosphere by the reaction of ozone with nitrogen dioxide.¹ Although NO_3 is readily photolysed in the daytime, it can build up at night to a concentration of $\text{ca. } 10^9 \text{ molecule cm}^{-3}$ in the urban troposphere. Significant reaction may then occur with volatile organic compounds from both man-made and natural sources. The oxidation of simple alkanes and halogenated alkanes by NO_3 proceeds initially by H-atom abstraction with the formation of an alkyl radical and nitric acid. The atmospheric implications of such reactions for alkanes in terms of HNO_3 production have already been discussed.²

Here, a novel stopped-flow technique was used to make absolute determinations of rate constants in the range 10^{-15} – $10^{-18} \text{ cm}^3 \text{ molecule}^{-1} \text{ s}^{-1}$ for the overall interactions of NO_3 with ethane, propane, 2-methylpropane (isobutane) acetone, dichloromethane and chloroform and of the primary rate constant for the addition of NO_3 to ethene. As a result of the long contact times used (tens of seconds), detailed consideration has been given to NO_3 losses occurring by the fast secondary reactions which follow alkyl radical formation and also occurring heterogeneously. The small rate constants found for the H-atom abstractions confirm that these reactions are not of major importance for NO_3 loss in the troposphere, but the overall rate constants obtained do lend support to ideas on the relationship between the structure of the organic compounds and their reactivity towards the nitrate radical.

Experimental

Apparatus

A schematic diagram of the stopped-flow apparatus used is shown in Fig. 1. The diluent gas was helium (B.O.C. grade A), which was passed through an 'Oxisorb' (Messer Griesheim) trap before introduction at atmospheric pressure into the gas-handling system. A small part of the main flow was diverted through a bubbler containing a 2 : 1 mixture (by volume) of concentrated sulphuric and nitric acids held at $\text{ca. } 260 \text{ K}$ by an ethane-1,2-diol slush bath. The emerging anhydrous HNO_3 vapour reacted with F atoms to form the NO_3 radical and the unreactive product HF. The F atoms themselves

were formed by passing a mixture of $\text{ca. } 0.5\% \text{ CF}_4$ (B.O.C., >99%) in He through a 2450 MHz microwave discharge (50 W, Microtron 2000 source). CF_4 was chosen rather than F_2 as the source because of the greater ease of handling and purification (by trap-to-trap distillation). It was mixed in a bulb with He to $\text{ca. } 5\%$ by volume. All flows were controlled by needle valves (Nupro S series) and all except that of the co-reactant were measured by suitable ball flowmeters (RS Meterate series). The species that was to react with NO_3 was added through a calibrated capillary flowmeter. Measurement of the back pressure in the reactant bulb by a spoon gauge,³ and of the pressure difference across the capillary by a differential capacitance manometer (MKS Baratron 170M), allowed the flow rate of the reactant to be calculated. Cell pressures in the range 6.5–8.5 Torr† were measured by a pressure transducer (MKS Baratron 122A). The custom-built glass solenoid valves have already been described in detail.⁴ After establishing known steady-state concentrations of NO_3 and reactant, the valves were used to isolate a portion of the

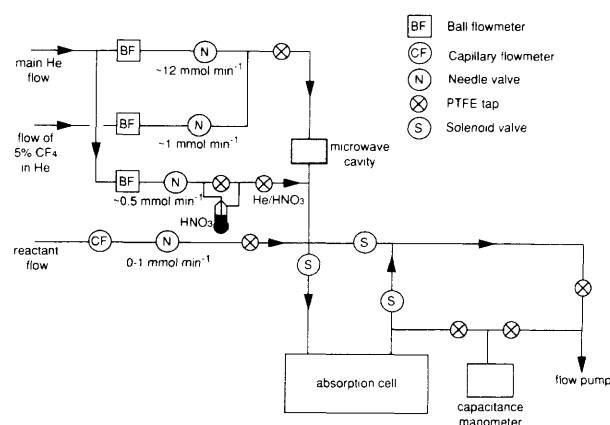


Fig. 1 The gas-handling apparatus

† 1 Torr = 101 325/760 Pa.

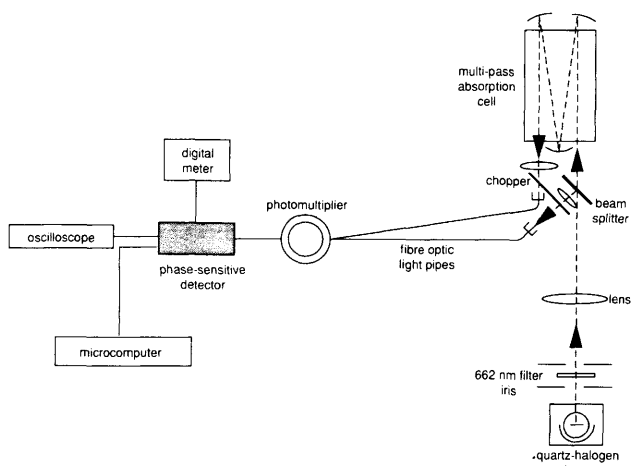


Fig. 2 The detection system, incorporating 12 optical passes through a cell 25.2 cm in length and 5.5 cm i.d. An earlier system had a smaller cell (30.0 cm, 3.6 cm) with only two passes

gas mixture in the cell and simultaneously to divert the main flow to the pump. The cell was coated with halocarbon wax.

Detection System

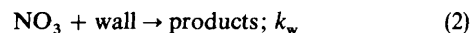
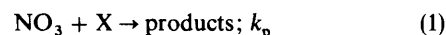
The NO_3 in the cell was detected by its optical absorption at $\lambda = 662 \text{ nm}$, a suitable collimated light beam being provided by the arrangement of the quartz-halogen bulb (150 W, Wotan), $\lambda = 661.8 \text{ nm}$ interference filter (3 nm fwhm, Ealing), lens and irises shown schematically in Fig. 2. Multi-pass optics permitted 12 passes through a 25.2 cm long, 5.5 cm i.d. cell. The reference beam and emerging sample beams were chopped alternately at 350 Hz before being guided onto the photomultiplier (EMI 9781R) via fibre-optic light pipes. The processing of the photomultiplier signal by the phase-sensitive detector and the method for recording the decay of the NO_3 signal on stopping the flow have been described previously.⁴ The maximum concentrations of NO_3 detected (before stopping the flow through the cell) were in the range $(2.0\text{--}5.0) \times 10^{13} \text{ molecule cm}^{-3}$, as calculated using the Beer-Lambert law. The effective absorption cross-section used was $8.9 \times 10^{-18} \text{ cm}^2 \text{ molecule}^{-1}$, a value measured by the NO titration method.¹ Noise on the decay traces with the 2 Hz filter and with five co-additions corresponded to ca. $2 \times 10^{11} \text{ molecule cm}^{-3}$. In an earlier implementation, a smaller cell, 30.0 cm long and 2.6 cm i.d., with larger surface-to-volume ratio, was used with only two optical passes; effective noise levels in this arrangement corresponded to ca. $4 \times 10^{11} \text{ molecule cm}^{-3}$.

Experiments using the arrangement with two optical passes were carried out to investigate the reactions of NO_3 with ethane (BDH), chloromethane (BDH), dichloromethane (BDH), chloroform (BDH) and acetone (BDH). The system with 12 passes has since been used to measure the rates of reaction with ethene (BDH), propane (BOC) and isobutane (BDH). All these reagents had a purity of >99%. Further purification was achieved by distillation using a liquid- N_2 trap or appropriate slush bath.

Data Analysis and Results

All reactions were studied under pseudo-first-order conditions, the decay of NO_3 being recorded in the presence of an excess (at least tenfold) of organic reactant, X. The loss of NO_3 in reaction with X and with the wall was assumed to be

represented by the equations



where k_p is the second-order rate constant for the primary step and k_w is the overall first-order rate constant for the wall reaction.

The integrated form of the rate equation for these processes is then

$$-\ln([\text{NO}_3]_t/[\text{NO}_3]_0) = (k_w + sk_p[\text{X}])t = k't \quad (3)$$

where t is the time elapsed after stopping the flow and s , the stoichiometric factor, is the number of NO_3 molecules consumed for every X molecule reacting initially; s thus allows for secondary reactions between NO_3 and the products of the primary and any subsequent steps. $[\text{NO}_3]_0$ is the averaged steady-state concentration in the flow through the cell, $[\text{X}]$ is effectively the known initial concentration of reactant X (since there is negligible loss of reactant over time t) and k' is the pseudo-first-order rate constant. $\ln([\text{NO}_3]_t/[\text{NO}_3]_0)$ was calculated for each data point in a chosen time interval of the decay and k' was obtained by linear least-squares analysis. A further linear least-squares treatment, of the relationship between k' and $[\text{X}]$, was used to extract sk_p and k_w .

Wall Reaction

Typical decays of NO_3 in the smaller and larger cells, in the absence of added reactant, are shown in Fig. 3. The initial rapid drop in signal over the first second or so was presumed to be due to the relatively fast reaction with some NO_2 initially present (as a result of HNO_3 decomposition) to form N_2O_5 .⁵ The N_2O_5 is stable for the conditions obtaining in the cell (see later). For the remainder of the decay, there was no evidence with either cell for any second-order loss of NO_3 , resulting, for example, from reaction of NO_3 with itself; plots of $\ln([\text{NO}_3]_t/[\text{NO}_3]_0)$ against t for $t = 2\text{--}20 \text{ s}$ were linear, with the slopes yielding first-order rate constants for the smaller and larger cells of (0.073 ± 0.002) and $(0.049 \pm 0.001) \text{ s}^{-1}$ (95% confidence limits). The assumption that the first-order loss of NO_3 was due entirely to a wall reaction was supported by the difference in the value of k_w for the two cells which reflected their different surface-to-volume

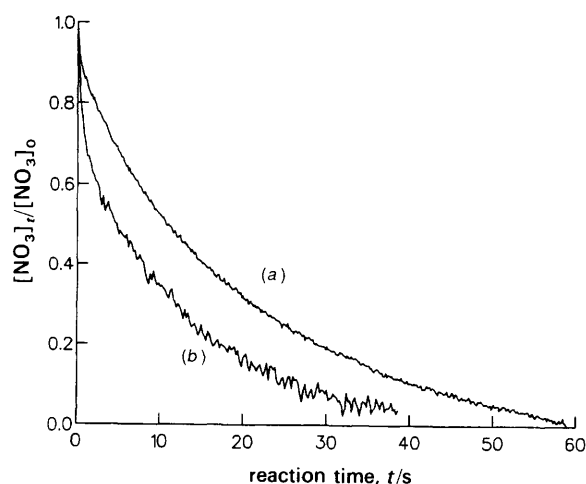
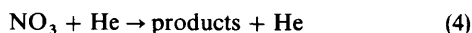


Fig. 3 Decays of NO_3 alone in (a) the large cell [surface-to-volume ratio ($S:V$) = 0.73, $k_w = 0.049 \text{ s}^{-1}$, 12 passes]; (b) the small cell ($S:V$ = 1.11, $k_w = 0.074 \text{ s}^{-1}$, 2 passes). In both cases, $[\text{NO}_3]_0 = 3.7 \times 10^{13} \text{ molecule cm}^{-3}$

ratios (0.73 and 1.11 for the larger and smaller cell). Also, another possible first-order loss



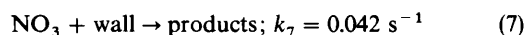
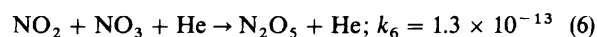
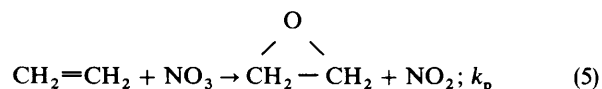
does not appear to contribute, since no increase in the rate of loss of NO_3 was observed on increasing the pressure of helium in the cell. These decays also illustrate the considerable improvement in signal-to-noise ratio achieved by using the improved detection system with a much longer path-length (and incidentally greatly reduced vibrations).

Reaction with Ethene

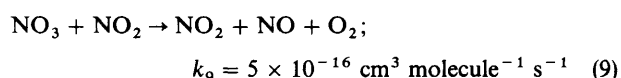
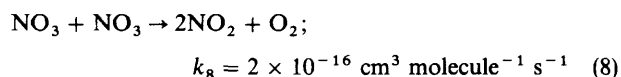
Fig. 4 shows some of the recorded decays of NO_3 in the presence of known concentrations of ethene, obtained using the larger cell. Analysis of these data to find k' for each decay and then plotting against $[\text{C}_2\text{H}_4]$ (see Fig. 5), yielded values for sk_p and k_w of $(3.2 \pm 0.3) \times 10^{-16} \text{ cm}^3 \text{ molecule}^{-1} \text{ s}^{-1}$ and $(0.042 \pm 0.011) \text{ s}^{-1}$, respectively. The quoted errors in these rate constants include only the 95% confidence limits of the linear least-squares analysis and do not allow for possible systematic errors in the measured $[\text{C}_2\text{H}_4]$ values used. The rate constant for wall loss agreed within error with the value of $(0.046 \pm 0.004) \text{ s}^{-1}$ obtained by averaging the individual

values measured from decays of NO_3 alone. This agreement suggests that there is no significant surface reaction involving ethene (unless, of course, the rate of any heterogeneous reaction of NO_3 with ethene is proportional to $[\text{C}_2\text{H}_4]$).

A numerical integration program was then used to simulate individual NO_3 decays. The reactions of importance in the system are



where the second-order and pseudo-second-order rate constants for reactions (5) and (6) have the units $\text{cm}^3 \text{ molecule}^{-1} \text{ s}^{-1}$. The value used for k_6 was that measured by Smith *et al.*⁵ for 298 K and 8 Torr of He. The reverse of reaction (6), having a rate constant of $4 \times 10^{-3} \text{ s}^{-1}$ (calculated using the average equilibrium constant suggested by Wayne *et al.*¹), can be omitted from the reaction scheme without affecting the shape of the simulated decay. Other reactions whose inclusion were found to make no difference to the predicted concentration and which were thus discounted include



reactions for which rate constants are already known.^{6,7}

Ethylene oxide rather than acetaldehyde was assumed to be the product eventually formed following addition of electrophilic NO_3 to the π -bond of the alkene. Dlugokencky and Howard⁸ have shown that the channel most thermodynamically favoured for the decomposition of the excited $\text{CH}_3\text{CHCH}_2\text{ONO}_2$ intermediate formed from propene is, in fact, to the aldehyde, with the expulsion of a molecule of NO_2 . However, formation of the epoxide is favoured kinetically because the activation energy required for H-atom transfer in going from the adduct to propanal is not available. Extension of these principles to the ethene- NO_3 system suggests that there is negligible formation of acetaldehyde and certainly no subsequent further loss of NO_3 . Indeed, the rate constant for the reaction of NO_3 with $\text{CH}_3\text{CH}=\text{O}$ is only⁸ ca. $3 \times 10^{-15} \text{ cm}^3 \text{ molecule}^{-1} \text{ s}^{-1}$. Also, the epoxide itself could be expected to be stable towards NO_3 even over our very long contact times, simply by analogy with the relatively slow rates of H-atom abstraction from ethane and acetone (see later). Only the NO_2 which is formed in the primary step (5) is thus likely to be responsible for secondary removal of NO_3 in reaction (6).

The experimental data appear to obey pseudo-first-order kinetics after an initial rapid decay resulting from chemistry of the NO_3 precursors. The simulated data were tested for first-order behaviour by fitting them to the experimental points after the initial decay, plotted as $\ln([\text{NO}_3]/[\text{NO}_3]_0)$ against time. A modification of a least-squares fitting procedure was then used to match experiment and prediction. The best fit for a chosen decay was with $k_p = (1.7 \pm 0.5) \times 10^{-16} \text{ cm}^3 \text{ molecule}^{-1} \text{ s}^{-1}$ at 300 K, where the error includes allowances for maximum possible systematic and random errors in the values of $[\text{C}_2\text{H}_4]$ and k_w used in the model. The stoichiometric factor for our reaction system was therefore ca. 1.9. Recently published values of k_p for reaction (5) at room temperature are⁹ $(2.14 \pm 0.32) \times 10^{-16}$ and¹⁰ $(1.85 \pm 0.24) \times 10^{-16} \text{ cm}^3 \text{ molecule}^{-1} \text{ s}^{-1}$ using relative rate

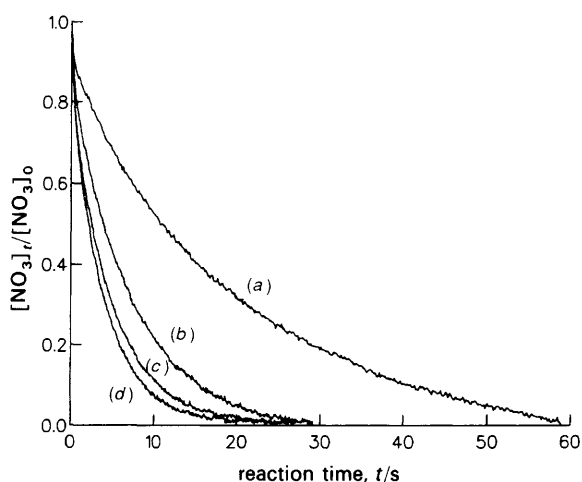


Fig. 4 Decays of NO_3 on reaction with (a) 0; (b) 2.72; (c) 4.80; (d) $6.08 \times 10^{14} \text{ molecule cm}^{-3}$ of ethene

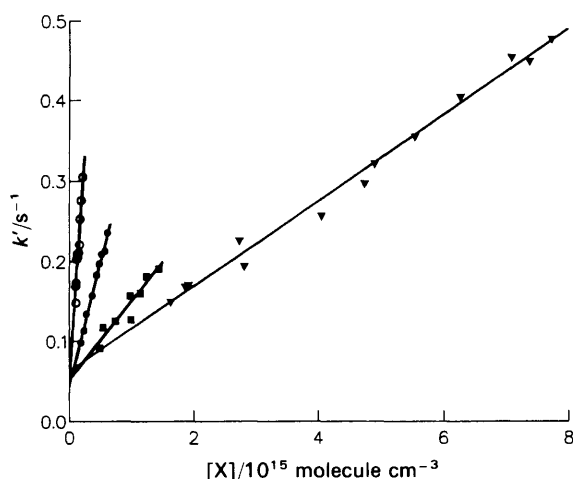
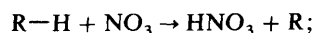


Fig. 5 Plots of the pseudo-first-order rate constant for NO_3 loss, k' , against concentration of organic reactant, $[\text{X}]$, where X (RH for abstraction reactions) is ∇ , C_2H_6 ; \blacksquare , C_3H_8 ; \bullet , C_2H_4 ; \circ , $i\text{-C}_4\text{H}_{10}$

and discharge-flow techniques, respectively. This good agreement with the literature supports our view that there is no significant heterogeneous reaction.

Reaction with Alkanes and Chlorinated Alkanes

The stopped-flow technique and data analysis described above were used to investigate the reactions at room temperature of the nitrate radical with a series of simple alkanes and chlorinated methanes, RH, in which the primary step in the system was the abstraction of a hydrogen atom to form nitric acid and a (chloro)alkyl radical, R



$$k_p < 10^{-15} \text{ cm}^3 \text{ molecule}^{-1} \text{ s}^{-1} \quad (10)$$

Plots of k' against $[\text{RH}]$, for those compounds studied where a definite reaction was detected, are included in Fig. 5 and 6. The slopes of these plots give the overall rate constants for the reaction systems as shown in Table 1, where the errors again only include the 95% confidence limits of the calculated slope. In all cases, the value of k_w (the intercepts in Fig. 5 and 6) agreed within statistical error with the measured rate constant for the loss of NO_3 in the absence of reactant. This agreement confirmed again that the addition of reactant to the system did not significantly alter the rate at which NO_3 decayed on the halocarbon wax surface. It can also be seen that all plots for a particular cell have the same intercept irrespective of the nature of the reactant (namely 0.07 s^{-1} for the smaller cell and 0.05 s^{-1} for the larger one). For isobutane, $[\text{i-C}_4\text{H}_{10}]_0/[\text{NO}_3]_0$ was in the range 5–10 rather than ≥ 10 as ideally required for the pseudo-first-order treatment of data. However, the large value of s involved in our

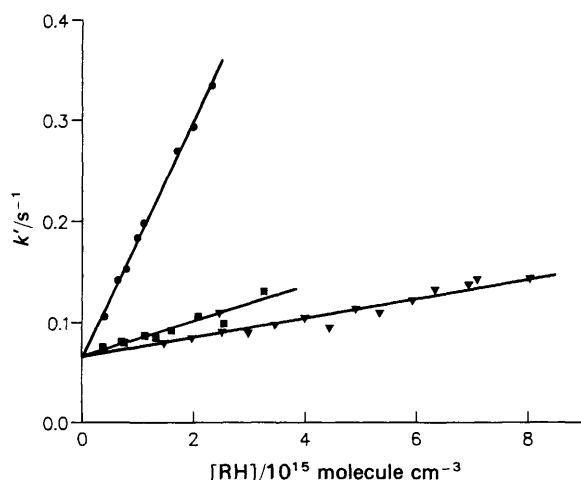


Fig. 6 Plots of pseudo-first-order rate constant for NO_3 loss, k' , against concentration of organic reactant, $[\text{RH}]$, where RH is ▼, CH_2Cl_2 ; ■, $(\text{CH}_3)_2\text{C}=\text{O}$; ●, CHCl_3 .

Table 1 Overall rate constants for the reaction of NO_3 with selected organic species

reactant	T/K	$sk_p/10^{-17} \text{ cm}^3 \text{ molecule}^{-1} \text{ s}^{-1}$	cell
C_2H_6	302	5.4 ± 0.4	small
C_3H_8	298	9.6 ± 3.3	large
$\text{i-C}_4\text{H}_{10}$	298	120 ± 20	large
CH_2Cl_2	300	0.96 ± 0.19	small
CHCl_3	304	12 ± 1	small
$(\text{CH}_3)_2\text{C}=\text{O}$	302	1.7 ± 0.5	small
CH_4	302	≤ 0.08	small
CH_3Cl	300	≤ 0.1	small

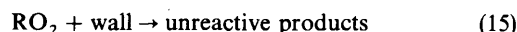
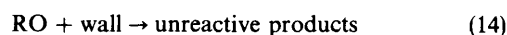
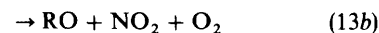
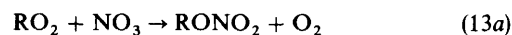
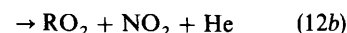
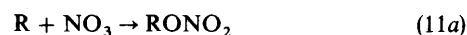
system (see later) means that even in the worst case, $[\text{i-C}_4\text{H}_{10}]$ decreased by less than 2% during the measurement period.

In experiments carried out with methane and chloromethane, no significant increase in the value of k' above the rate constant for wall loss in the absence of reactant was found. Assuming that an increase in k' of at least 0.02 s^{-1} would be detectable over the concentration range investigated, then upper limits of the values of sk_p for the reaction of CH_4 and CH_3Cl with NO_3 could be estimated to be $8 \times 10^{-19} \text{ cm}^3 \text{ molecule}^{-1} \text{ s}^{-1}$ and $1 \times 10^{-18} \text{ cm}^3 \text{ molecule}^{-1} \text{ s}^{-1}$ as indicated in Table 1.

Discussion

Secondary Reactions and Modelling

The secondary reactions involved in alkane- NO_3 systems have been discussed in detail by Bagley *et al.*² for a discharge-flow system with contact times up to ca. 0.5 s. The effect of these reactions on the decay of NO_3 is even more pronounced in our stopped-flow experiments because of the very long reaction times involved. The modelling procedure used to obtain the best fit between the experimental and simulated data was similar to that used for the ethene- NO_3 system. In the alkane- NO_3 systems investigated, the most important reactions following alkyl radical formation in reaction (10) were

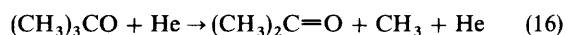


The total rate constant for reaction (11), k_{11} , used in the model was taken as $2.5 \times 10^{-11} \text{ cm}^3 \text{ molecule}^{-1} \text{ s}^{-1}$ by analogy with the reaction of NO_2 with CH_3 . k_{13} was taken as $10^{-13} \text{ cm}^3 \text{ molecule}^{-1} \text{ s}^{-1}$ since, although the original measurements of Crowley *et al.*¹² indicated a value of ca. $4 \times 10^{-13} \text{ cm}^3 \text{ molecule}^{-1} \text{ s}^{-1}$ for $\text{R} = \text{C}_2\text{H}_5$ (20 Torr, 298 K), a revised value of $1.2 \times 10^{-13} \text{ cm}^3 \text{ molecule}^{-1} \text{ s}^{-1}$ or lower has been suggested (J. P. Burrows, personal communication). k_{12} was taken as ca. $4 \times k_{13}$ by analogy with the ratio of rate constants¹³ for the reactions of NO_2 with RO and RO_2 . Such approximations of rate constants in the model are acceptable, even allowing that k_{13} (and hence k_{12}) may be smaller for larger R species, because the fits to the experimental decays were relatively insensitive to their values. The lack of sensitivity depends on k_{11} being large enough to ensure a steady state for $[\text{R}]$, and on k_{13} being less than $10^{-12} \text{ cm}^3 \text{ molecule}^{-1} \text{ s}^{-1}$. However, the fits were very sensitive to the branching ratios of these three reactions and, in particular, to $f_{11} [= k_{11a}/(k_{11a} + k_{11b})]$. Since there appears to be no experimental determination of these ratios for any of the relevant R, RO and RO_2 species, it is impossible to extract k_p from the numerical modelling of the reaction systems; a whole range of k_p values gave equally good fits, depending on the values of f_{11} , f_{12} and f_{13} chosen. Furthermore, k_{14} and k_{15} had to be in the range $5\text{--}10 \text{ s}^{-1}$ if they were not to affect the fit significantly. Fits were quite sensitive to the value of k_w , but this rate constant was determined

accurately enough for any error not to affect greatly the derived value of k_p . Thus, what can be deduced with certainty is that the stoichiometric factor is ≥ 2 (the value of 2 itself corresponding to complete formation of the stable peroxy adduct, with $f_{11} = 1$). By halving the overall rate constants given in Table 1, an upper limit for k_p is therefore obtained.

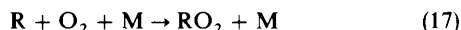
If all the branching ratios are set equal to zero in the model, the effects of secondary radical reactions are maximized, and an attempt can be made at estimating the lower limit for k_p . With k_{14} and k_{15} varied between 5 and 10 s^{-1} , and again allowing for possible errors in the $[\text{RH}]$ and k_w values used in the model, the minimum value of k_p which gave a good fit was found to be $(1.1 \pm 0.2) \times 10^{-17} \text{ cm}^3 \text{ molecule}^{-1} \text{ s}^{-1}$ for reaction with ethane (corresponding to a maximum value for the stoichiometric factor of ca. 5) and $(2.2 \pm 0.2) \times 10^{-17} \text{ cm}^3 \text{ molecule}^{-1} \text{ s}^{-1}$ for reaction with propane (maximum $s \approx 4$).

With isobutane, there were further complications in the modelling of the reactions which meant that there could be no real confidence in any lower limits for k_p obtained. For the reaction of isobutane with NO_3 , the measured overall rate constant, when compared with the value of Bagley *et al.*² for k_p of $1.1 \times 10^{-16} \text{ cm}^3 \text{ molecule}^{-1} \text{ s}^{-1}$, suggests a stoichiometric factor of ca. 11 for our system. On putting this value of k_p into the model, however, the simulated decay was always considerably slower than that observed experimentally, even with all branching ratios set to 0. The reaction missing in our model was thought to be



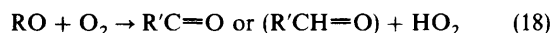
where k_{16} was estimated to be $150\text{--}200 \text{ s}^{-1}$ for our pressure, temperature and buffer gas (by analogy with the data of Batt *et al.*¹⁴ who found a value of 305 s^{-1} at 10 Torr and 303 K with CF_4 as a third body). Although the uncertainty in k_{16} , and even in the reaction pathway, precludes fitting to obtain a rate constant, it is possible to obtain a reasonable match with the experimental data. The omission from the model for the reaction of NO_3 with ethane of the ethoxy radical decomposition analogous to reaction (16) is not significant, because of a rate constant of much less than 1 s^{-1} for $\text{R} = \text{C}_2\text{H}_5$.¹⁵ For propane, the equivalent reaction is also unimportant, the rate constant having been measured¹⁵ to be 2.7 s^{-1} at 300 K in 1 atm† of air. With a value of 1 s^{-1} (taken as reasonable for 8 Torr of He), no significant difference in the value of k_p was required to give the 'best' fit, compared to that value of k_p required with a rate constant of zero. An additional possible complication in this system is that the acetaldehyde formed could react significantly with NO_3 . This process is assumed to be unimportant in the isobutane system since the rate constant for the reaction of NO_3 with $(\text{CH}_3)_2\text{C}=\text{O}$ was found to be only $\leq 1.7 \times 10^{-17} \text{ cm}^3 \text{ molecule}^{-1} \text{ s}^{-1}$ (see later) compared to⁸ ca. $3 \times 10^{-15} \text{ cm}^3 \text{ molecule}^{-1} \text{ s}^{-1}$ for the reaction of NO_3 with $\text{CH}_3\text{CH}=\text{O}$.

Experiments were carried out with ethane and propane in the presence of molecular oxygen (B.O.C. industrial grade) to try to gain some insight into the relative values of the branching ratios f_{11} , f_{12} and f_{13} for each of these two reaction systems. With sufficient oxygen present, then following reaction (10), the direct formation of alkylperoxy radicals by the step



should bypass reaction (11) completely, leading to an NO_3 -destruction cycle which starts with reaction (13). However, the subsequent loss of NO_3 can occur not only in

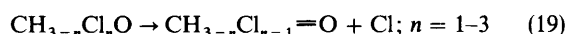
reaction (12), with the regeneration of RO_2 , but also following the reaction of RO with more oxygen in the process



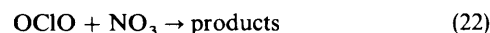
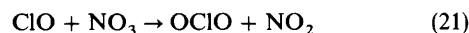
Formation of HO_2 will lead to the destruction of several more NO_3 molecules in competition with the main cycle of reactions (12) and (13).

For the ethane system, with 0.5–2.9, 0.4–2.4 and $0.04 \times 10^{15} \text{ molecule cm}^{-3}$ for the initial concentrations of C_2H_6 , O_2 and NO_3 , the measured sk_p was $(4.6 \pm 1.0) \times 10^{-17} \text{ cm}^3 \text{ molecule}^{-1} \text{ s}^{-1}$, a value that does not differ significantly from that obtained in the absence of oxygen. For $\text{R} = \text{C}_2\text{H}_5$, then with a recommended value¹³ for k_{17} of $5 \times 10^{-12} \text{ cm}^3 \text{ molecule}^{-1} \text{ s}^{-1}$ at the high-pressure limit (compared to¹¹ ca. $2.5 \times 10^{-11} \text{ cm}^3 \text{ molecule}^{-1} \text{ s}^{-1}$ for k_{11}), the relative concentrations mean that the majority of the ethyl radicals will react with O_2 rather than with NO_3 . That there is no increase in the measured stoichiometric factor upon forming $\text{C}_2\text{H}_5\text{O}_2$ directly, rather than *via* reactions (11) and (12), suggests that f_{11} is likely to be small in comparison with f_{12} and f_{13} . However, with propane as reactant, the overall rate constant increased from (1.0 ± 0.4) to $(2.7 \pm 0.6) \times 10^{-16} \text{ cm}^3 \text{ molecule}^{-1} \text{ s}^{-1}$ for C_3H_8 , O_2 and NO_3 concentrations of (0.1–0.7), (0.4–2.8) and $0.02 \times 10^{15} \text{ molecule cm}^{-3}$. Thus, even though k_{17} is three times larger¹⁴ for $\text{R} = i\text{-C}_3\text{H}_7$ than for C_2H_5 (whilst k_{18} has the same value for both radicals¹³ of $8 \times 10^{-15} \text{ cm}^3 \text{ molecule}^{-1} \text{ s}^{-1}$), the threefold increase in s for the reaction indicates that f_{11} favours the stable adduct whereas f_{12} and f_{13} favour the radical product channels. Much faster generation of $i\text{-C}_3\text{H}_7\text{O}$ by reaction (13) when O_2 is present leads to more NO_3 loss cycles that can start with reaction (12) or indirectly with reaction (18).

For the NO_3 -chlorinated methane reaction systems, the decomposition of the chlorinated alkoxy species [formed in reaction (11b)] may lead to an important difference in the secondary chemistry, provided that chlorine-atom production by the reaction



is sufficiently fast for the processes



to compete for NO_3 with reaction (13). There has been no direct measurement or estimation of k_{19} for any of the chlorinated methanes, so that the importance of this reaction in the model cannot be assessed.

Comparisons and Trends

A comparison of the upper limits (obtained from either measured sk_p values or noise levels) with literature values for the rate constants is given in Table 2.

It can be seen that our value is no improvement on the previous best upper limit for the reaction with CH_4 measured by Cantrell *et al.*,¹⁶ who used a static reactor with relative-rate technique.

The lower limit suggested for the rate constant of reaction with ethane is tentative but is nevertheless much higher than both the other suggested upper limit of Wallington *et al.*¹⁷ and the value for k_p from Bagley *et al.*² of $2 \times 10^{-18} \text{ cm}^3 \text{ molecule}^{-1} \text{ s}^{-1}$, although the latter does involve a long extrapolation from higher temperatures. This apparent disagreement strongly suggests that an Arrhenius plot for ethane

† 1 atm = 101 325 Pa.

Table 2 Comparison between our upper limits and literature values for k_p

reactant	$k_p/10^{-17} \text{ cm}^3 \text{ molecule}^{-1} \text{ s}^{-1}$		ref.
	this work	literature	
CH ₄	$\leq 0.08^a$	≤ 0.0006	16
C ₂ H ₆	$\leq 2.7 \pm 0.2$	≤ 0.4	17
		0.2	2
C ₃ H ₈	$\leq 4.8 \pm 1.7$	—	—
i-C ₄ H ₁₀	$\leq 60 \pm 10$	9.7 ± 2.5	9
		11 ± 2	2
(CH ₃) ₂ C=O	$\leq 0.85 \pm 0.25$	≤ 300	18
CH ₃ Cl	$\leq 0.1^a$	1.57 ± 0.11	19
CH ₂ Cl ₂	$\leq 0.48 \pm 0.10$	1.66 ± 0.16	19
CHCl ₃	$\leq 6.0 \pm 0.5$	1.36 ± 0.17	19
		≤ 8.2	20

^a Upper limits determined from noise levels where no reaction is detectable; other limits are obtained by dividing the measured sk_p values by 2.

will, at lower temperatures, show deviation from the linearity observed at the higher temperatures (453–553 K) in the work of Bagley *et al.*² It is therefore of interest to estimate Arrhenius parameters for the abstraction of primary hydrogen atoms more appropriate to lower temperatures. There should be no problem with the Arrhenius parameters of Bagley *et al.* for secondary and tertiary H-atom abstractions since they were derived directly from low-temperature data. An Evans–Polanyi calculation can be used to estimate the activation energy for abstraction of a primary hydrogen atom. The activation energies for *n*-butane and isobutane are² 27.0 and 24.6 kJ mol⁻¹, and the enthalpies of reaction, ΔH_r , are²¹ -18.7 and -28.4 kJ mol⁻¹. For ethane, ΔH_r is²¹ -8.2 kJ mol⁻¹, so that an Evans–Polanyi calculation suggests an activation energy of 29.6 kJ mol⁻¹ in this case where all hydrogens are primary. This activation energy may be compared with 36.8 kJ mol⁻¹ from Bagley *et al.* The range of values for $k(300 \text{ K})$ from the present work is $(1.1\text{--}2.7) \times 10^{-17} \text{ cm}^3 \text{ molecule}^{-1} \text{ s}^{-1}$, so that the pre-exponential factor, A , is in the range $(1.6\text{--}3.8) \times 10^{-12} \text{ cm}^3 \text{ molecule}^{-1} \text{ s}^{-1}$. The correlation proposed in the recent review¹ favours the lower of the rate constants, suggesting a value of A for the abstraction of a single primary H atom of $2.6 \times 10^{-13} \text{ cm}^3 \text{ molecule}^{-1} \text{ s}^{-1}$. This estimate is more consistent with the pre-exponential factors for secondary and tertiary H-atom abstraction of Bagley *et al.*, of $6.3 \times 10^{-13} \text{ cm}^3 \text{ molecule}^{-1} \text{ s}^{-1}$ and $2.3 \times 10^{-12} \text{ cm}^3 \text{ molecule}^{-1} \text{ s}^{-1}$, than with their value of $9.5 \times 10^{-13} \text{ cm}^3 \text{ molecule}^{-1} \text{ s}^{-1}$ for a primary hydrogen atom and obtained by extrapolation from high-temperature data.

The value of k_p for the reaction of isobutane with NO₃ has been quite well determined, with recent relative-rate⁹ and discharge-flow² studies suggesting an average value of $1 \times 10^{-15} \text{ cm}^3 \text{ molecule}^{-1} \text{ s}^{-1}$. As has been discussed already, a large stoichiometric factor exists in our reaction system if the literature value of k_p is correct, but the factor can at least be explained by the inclusion of reaction (16) in the model. However, it is also clear that the stopped-flow technique, with its very large contact time, is not the most suitable for study of the isobutane system.

The present work includes the first investigation of the reaction of NO₃ with propane. Using rate constants of $1.1 \times 10^{-17} \text{ cm}^3 \text{ molecule}^{-1} \text{ s}^{-1}$ from Bagley *et al.*² and $1.8 \times 10^{-18} \text{ cm}^3 \text{ molecule}^{-1} \text{ s}^{-1}$ from this work for the abstraction of a secondary H atom from butane and a primary H atom from ethane, the predicted rate constant for the reaction with propane is $3.3 \times 10^{-17} \text{ cm}^3 \text{ molecule}^{-1} \text{ s}^{-1}$,

which suggests a stoichiometry of 2–4 in our reaction system. The Szabó–Bérces relation²² predicts an increase in activation energy approximately proportional to the bond dissociation energy for a series of closely related compounds so that the rate constants for these reactions should increase with decreasing bond dissociation energy. Thus, even allowing for a stoichiometric factor for the reaction with isobutane of up to twice that for ethane and propane, the trend in sk_p values still reflects the R–H bond dissociation energies of 411, 398 and 390 kJ mol⁻¹ for primary, secondary and tertiary H atoms²¹ (although the increasing pre-exponential factors, of course, also contribute to an increase in k_p).

The reaction of acetone with NO₃ was investigated primarily to confirm that reaction with the carbonyl compound formed in reaction (18) was slow enough to be omitted from modelling of the isobutane (or any other alkane) system. An upper limit was obtained for the primary rate constant much reduced from that of Wallington *et al.*¹⁸ The bond dissociation energy for a C–H bond in acetone²¹ is the same as that in ethane, suggesting that the carbonyl group does not increase the rate of abstraction. The threefold decrease in sk_p , compared to that for ethane is likely to result from different branching ratios (and hence s values), although different secondary chemistry for the acetonyl radical from that assumed in the model for alkyl radicals cannot be ruled out.

For the chlorinated methanes investigated, Table 1 indicates that the rate constant for the reaction with NO₃ increases with the degree of chlorine substitution (providing that s values are comparable). Again, this result is in accordance with decreasing C–H bond dissociation energies of²¹ 422, 415 and 401 kJ mol⁻¹ in chloromethane, dichloromethane and chloroform. The values of Carlier *et al.*¹⁹ for the rate constants for reaction of NO₃ with the chlorinated methanes, and obtained by a relative-rate technique, exhibit no real trend and certainly do not show the decrease in k_p for increasing chlorine substitution that we have predicted and observed. It is very likely that s values for the series vary enough for k_p to really be constant, or that our conclusions are jeopardized by a differing increase in surface reactivity with increasing concentration of the reactant. There is thus an obvious conflict with literature results. The other upper limit for the room-temperature rate constant for the reaction with chloroform is found by long extrapolation of the Arrhenius equation²⁰ down to 304 K.

The authors express their gratitude to Dr. P. Biggs, Dr. S. J. Smith and Ms. D. M. Joseph for the large part they played in the development and commissioning of the stopped-flow apparatus. A.A.B. thanks the S.E.R.C. for a maintenance grant and C.E.C.M. thanks the N.E.R.C. for support under grant number GR3/7105. Acknowledgement is also due to the C.E.C. for grant EV4V-0093-C, which provided partial support for this work.

References

- 1 R. P. Wayne, I. Barnes, P. Biggs, J. P. Burrows, C. E. Canosa-Mas, J. Hjorth, G. Le Bras, G. K. Moortgat, D. Perner, G. Poulet, G. Restelli and H. Sidebottom, *Atmos. Env.*, 1991, **25A**, 1.
- 2 J. A. Bagley, C. E. Canosa-Mas, M. R. Little, A. D. Parr, S. J. Smith, S. J. Waygood and R. P. Wayne, *J. Chem. Soc., Faraday Trans.*, 1990, **86**, 2109.
- 3 R. P. Wayne, *J. Phys. E*, 1981, **14**, 306.
- 4 P. Biggs, A. A. Boyd, C. E. Canosa-Mas, D. M. Joseph and R. P. Wayne, *Meas. Sci. Technol.*, in the press.
- 5 C. A. Smith, A. R. Ravishankara and P. H. Wine, *J. Phys. Chem.*, 1985, **89**, 1423.

- 6 R. A. Graham and H. S. Johnston, *J. Phys. Chem.*, 1978, **82**, 254.
- 7 J. Hjorth, F. Cappellani, C. Nielsen and G. Restelli, in *Mechanisms of Gas-phase and Liquid-phase Chemical Transformations in Tropospheric Chemistry*, ed. R. A. Cox, Air Pollution Report 17, EUR 12035, C.E.C., Brussels, 1988, p. 73.
- 8 E. J. Dlugokencky and C. J. Howard, *J. Phys. Chem.*, 1989, **93**, 1091.
- 9 R. Atkinson, S. M. Aschmann and J. N. Pitts Jr., *J. Phys. Chem.*, 1988, **92**, 3454.
- 10 C. E. Canosa-Mas, S. J. Smith, S. Toby and R. P. Wayne, *J. Chem. Soc., Faraday Trans. 2*, 1988, **84**, 247.
- 11 F. Yamada, I. R. Slagle and D. Gutman, *Chem. Phys. Lett.*, 1981, **83**, 409.
- 12 J. N. Crowley, J. P. Burrows, G. K. Moortgat, A. Mellouki, G. Poulet and G. LeBras, Abstract O7, XIth International Symposium on Gas Kinetics, Assisi, Italy, 2–7 September 1990.
- 13 R. Atkinson, D. L. Baulch, R. A. Cox, R. F. Hampson Jr., J. A. Kerr and J. Troe, *J. Phys. Chem. Ref. Data*, 1989, **18**, 881.
- 14 L. Batt, M. W. M. Hisham and M. MacKay, *Int. J. Chem. Kinet.*, 1989, **21**, 55.
- 15 A. C. Baldwin, J. R. Barker, D. M. Golden and D. G. Hendry, *J. Phys. Chem.*, 1977, **81**, 2483.
- 16 C. A. Cantrell, J. A. Davidson, R. E. Shetter, B. A. Anderson and J. G. Calvert, *J. Phys. Chem.*, 1987, **91**, 5858.
- 17 T. J. Wallington, R. Atkinson, A. M. Winer and J. N. Pitts Jr., *J. Phys. Chem.*, 1986, **90**, 4640.
- 18 T. J. Wallington, R. Atkinson, A. M. Winer and J. N. Pitts Jr., *J. Phys. Chem.*, 1986, **90**, 5393.
- 19 P. Carlier, H. Hannichi, A. Kartoudis, A. Martinet and L. Mouvier, in *Tropospheric NO_x Chemistry—Gas-phase and Multiphase Aspects*, ed. O. J. Nielsen and R. A. Cox, C.E.C. Research Report 9, EUR 11440, C.E.C. Brussels, 1987, p. 133.
- 20 C. E. Canosa-Mas, S. J. Smith, S. Toby and R. P. Wayne, *J. Chem. Soc., Faraday Trans. 2*, 1989, **85**, 709.
- 21 D. F. McMillen and D. M. Golden, *Annu. Rev. Phys. Chem.*, 1982, **33**, 493.
- 22 Z. G. Szabó and T. Bérces, *Z. Phys. Chem.*, 1968, **57**, 3.

Paper 1/01671G; Received 10th April, 1991